Cellular and Metabolic Engineering **Biotechnology and Bioengineering**
DOI 10.1002/bit.26281

An artificial TCA cycle selects for efficient α-ketoglutarate dependent hydroxylase catalysis in engineered *Escherichia coli*†

Running Title: Strain design for proline hydroxylation *in vivo*

Eleni Theodosiou[1], Marina Breisch[2], Mattijs K. Julsing[2], Francesco Falcioni[2,†], Bruno Bühler[1*], and Andreas Schmid[1]

[1]Department of Solar Materials, Helmholtz Centre for Environmental Research-UFZ, Permoserstr. 15, 04318 Leipzig, Germany; telephone: +49-341-235-4687; fax: +49-341-23545-1246; e-mail: bruno.buehler@ufz.de

[2]Laboratory of Chemical Biotechnology, Department of Biochemical and Chemical Engineering, TU Dortmund University, Dortmund, Germany

†Current Address: Hypha Discovery Ltd, The Russell Building, Brunel Science Park, Uxbridge, Middlesex UB8 3PQ, United Kingdom

[*]*Correspondence to*: Bruno Bühler

†This article has been accepted for publication and undergone full peer review but has not been through the copyediting, typesetting, pagination and proofreading process, which may lead to differences between this version and the Version of Record. Please cite this article as doi: [10.1002/bit.26281]

Additional Supporting Information may be found in the online version of this article.

Received December 20, 2016; Revision Received February 13, 2017; Accepted March 01, 2017

Abstract

Amino acid hydroxylases depend directly on the cellular TCA cycle via their cosubstrate *a*-ketoglutarate (α-KG) and are highly useful for the selective biocatalytic oxyfunctionalization of amino acids. This study evaluates TCA cycle engineering strategies to force and increase α-KG flux through proline-4-hydroxylase (P4H). The genes *sucA* (α-KG dehydrogenase E1 subunit) and *sucC* (succinyl-CoA synthetase β subunit) were alternately deleted together with *aceA* (isocitrate lyase) in proline degradation-deficient *Escherichia coli* strains (Δ*putA*) expressing the *p4h* gene. Whereas the Δ*sucC*Δ*aceA*Δ*putA* strain grew in minimal medium in the absence of P4H, relying on the activity of fumarate reductase, growth of the Δ*sucA*Δ*aceA*Δ*putA* strictly depended on P4H activity, thus coupling growth to proline hydroxylation. P4H restored growth, even when proline was not externally added. However, the reduced succinyl-CoA pool caused a 27% decrease of the average cell size compared to the wildtype strain. Medium supplementation partially restored the morphology and, in some cases, enhanced proline hydroxylation activity. The specific proline hydroxylation rate doubled when *putP*, encoding the Na^+/L-proline transporter, was overexpressed in the Δ*sucA*Δ*aceA*Δ*putA* strain. This is in contrast to wildtype and Δ*putA* single-knock out strains, in which α-KG availability obviously limited proline hydroxylation. Such α-KG limitation was relieved in the Δ*sucA*Δ*aceA*Δ*putA* strain. Furthermore, the Δ*sucA*Δ*aceA*Δ*putA* strain was used to demonstrate an agar plate-based method for the identification and selection of active α-KG dependent hydroxylases. This together with the possibility to waive selection pressure and overcome α-KG limitation in respective hydroxylation processes based on living cells emphasizes the potential of TCA cycle engineering for the productive application of α-KG dependent hydroxylases. This article is protected by copyright. All rights reserved

Keywords: Whole-cell biocatalysis; TCA cycle engineering; α-KG dependent dioxygenase; L-proline transporter; proline hydroxylation.

Introduction

When recombinant microbial cells are employed for biotransformations, the operation and regulation of the cellular metabolic network are key players orchestrating catalytic efficiency. This interplay is tighter, when microbial metabolism supplies cosubstrates or redox cofactors required for activity (Blank et al., 2010; Falcioni et al., 2013; Schrewe et al., 2013; Theodosiou et al., 2015). The synthesis of hydroxylated amino acids using recombinant *Escherichia coli* cells is such a case, as employed hydroxylases typically depend on the cosubstrate α-ketoglutarate (α-KG), which is withdrawn from the host tricarboxylic acid (TCA) cycle (Hausinger, 2004). The central carbon metabolism fuels the enzyme with α-KG and in turn assimilates and recycles the coproduct of the enzymatic reaction, i.e., succinate. Metabolic engineering of such a whole-cell biocatalyst is highly attractive, not only for the construction of optimized cell factories for the synthesis of hydroxylated amino acids, but also for investigating metabolic responses upon the applied perturbations.

Smirnov et al. (2010) engineered *E. coli* MG1655 to produce *trans*-4-hydroxy-L-isoleucine, a natural non-proteinogenic amino acid with insulinotropic activity, from L-isoleucine using an α-KG dependent L-isoleucine-4-hydroxylase (IDO). The genes *sucAB* (encoding α-KG dehydrogenase) and *aceA* (encoding isocitrate lyase) were deleted aiming at a forced and increased carbon flux through IDO, restoring α-KG conversion into succinate and thus cyclic TCA flux. The *aceK* gene also was deleted considering that isocitrate dehydrogenase kinase/phosphatase (AceK) can inactivate isocitrate dehydrogenase and prevent α-KG synthesis. The mutant strain could not grow in minimal medium due to the broken TCA cycle, which was restored by the IDO activity enabling growth combined with the hydroxylation of L-isoleucine into *trans*-4-hydroxy-L-isoleucine at a molar yield of 82%. The interaction of the target reaction with host metabolism as well as the impact of the applied strain redesign on physiology and biocatalyst efficiency remained largely uncharacterized.

Additionally, it remains unclear, whether and how cell physiology and biocatalytic performance are affected by decreased succinyl-CoA (sucCoA) availability, which can be expected to accompany a *sucA* deletion. SucCoA is needed for lysine, methionine, and diaminopimelate biosynthesis, with the latter being essential for cell wall formation (**Supplemental Fig. S1**).

In this work, we tested the TCA cycle engineering strategy described above to produce *trans*-4-hydroxy-L-proline (hyp), a valuable chiral building block for the synthesis of pharmaceuticals (Hara and Kino, 2009) using an α-KG dependent L-proline-4-hydroxylase (P4H) in *E. coli*. For this purpose, we targeted oxidative TCA cycle and the glyoxylate shunt pathway in *E. coli* BL21(DE3)(pLysS), the optimal host strain for P4H synthesis (Falcioni et al., 2013). *SucA* (α-KG dehydrogenase E1 subunit) and *sucC* (sucCoA synthetase β subunit) were alternately deleted in combination with *aceA* (isocitrate lyase) (**Fig. 1**), in order to separately assess the effect of α-KG dehydrogenase or sucCoA synthetase deletion on host physiology. Deletion of *aceK* was not tackled, since it is known to be activated in *E. coli* under conditions not relevant for this study, e.g., during growth on acetate as the sole carbon source (Cozzone and El-Mansi, 2005). Intrinsic proline degradation was avoided by relying on a *putA* deletion mutant enabling a molar hyp yield of 100% on proline (Theodosiou et al., 2015). The resulting triple mutants Δ*sucA*Δ*aceA*Δ*putA* (referred to as 3Δ*sucA*) and Δ*sucC*Δ*aceA*Δ*putA* (referred to as 3Δ*sucC*) (**Fig. 1**) were characterized in terms of microbial physiology, metabolic resilience, and biocatalytic efficiency. Further, *putP* encoding the Na^+/L-proline transporter was overexpressed with the aim to probe and circumvent substrate uptake limitation. Besides hyp synthesis from L-proline, its synthesis directly from glucose (fermentative production) also was quantified and medium supplementations strategies were followed to investigate physiological effects of a potential sucCoA shortage. Finally, the 3Δ*sucA* strain was evaluated as a selection tool for α-KG dependent amino acid hydroxylases.

Materials and Methods

Chemicals

L-proline was kindly provided by Evonik Rexim SAS (Ham, France); all other chemicals were purchased from Sigma-Aldrich (Munich, Germany) or Carl-Roth (Karlsruhe, Germany) and were of the highest purity available.

Bacterial strains, plasmids, and cultivation conditions

The strains and plasmids used in this study are listed in **Table I**. For the *sucA*, *sucC*, and *aceA* gene deletions, the Quick & Easy *E. coli* Gene Deletion Kit by Red®/ET® Recombination (Gene Bridges GmbH, Heidelberg, Germany) was used. The gene *putP* (including 19 bp upstream of the ATG codon and the stop codon) was amplified by PCR from genomic DNA of *E. coli* BL21(DE3) using Phusion polymerase (Thermo Fisher Scientific, Schwerte, Germany) and cloned as a *Pst*I/*Bst*BI fragment in the pBAD/*Myc*-His vector (Thermo Fisher Scientific, Schwerte, Germany). The resulting plasmid pBAD-putP was used to transform *E. coli* DH5α by electroporation. The plasmid pEB-p4h1of-putP was constructed via Gibson assembly (Gibson et al., 2009) of PCR-fragments that were derived from pET-p4h1of (vector backbone) and pBAD-putP (*putP* expression cassette composed of *araC*, P_{bad}, and *putP*). The oligonucleotides used are listed in **Supplemental Table S2**.

Recombinant *E. coli* strains were routinely precultured in LB complex medium (Sambrook and Russell, 2001) and consecutively in M9 mineral medium containing 8.5 g L^{-1} $Na_2HPO_4 \cdot 2H_2O$, 3.0 g L^{-1} KH_2PO_4, 0.5 g L^{-1} NaCl, 1.0 g L^{-1} NH_4Cl, 2 mL L^{-1} 1M $MgSO_4$, 1 mg L^{-1} thiamine, 5 µg L^{-1} biotin, 1 mL L^{-1} US^{Fe} trace element solution (Bühler et al., 2003), 5 g L^{-1} glucose, and 5 mM proline (unless specified differently). If required, 34 mg L^{-1} chloramphenicol and 50 mg L^{-1} kanamycin were added. The same supplemented M9 medium also was used for subsequent main cultures. For the induction of *p4h1of* expression, 1 or 0.2 mM isopropyl-*β*-D-thiogalactopyranoside (IPTG) was added to both M9 preculture and main

culture at the time of inoculation, whereas 2 g L^{-1} arabinose were added for *putP* expression. All strains were incubated in baffled Erlenmeyer flasks in horizontal shakers at 30 °C and 250 rpm (INFORS HT, Bottmingen, Switzerland, Φ = 50 mm).

Analytical methods

Bacterial cell growth was monitored by measuring the optical density at 600 nm (OD_{600}), using a Libra S11 spectrophotometer (Biochrom Ltd., Cambridge, U.K.). The correlation factors between OD_{600} and cell dry weight (CDW) concentration (g_{cdw} L^{-1}) under the conditions studied were determined as described elsewhere (Blank et al., 2008) and are listed in **supplemental Table S3**. For the determination of consumption (glucose and L-proline) and production (acetate and hyp) rates, M9 cultures were sampled during exponential growth at regular intervals. After cell removal by centrifugation (10 min at 4 °C and 13,000g), glucose and acetate were separated and quantified with a LaChrom Elite® HPLC system (Hitachi Ltd. Corp., Tokyo, Japan) equipped with UV/VIS (λ=210nm) and refractive index (RID, VWR Hitachi L-2490) detectors using a Trentec 308R-Gel.H ion exclusion column (300 × 8 mm, Trentec Analysentechnik, Gerlingen, Germany) at 40 °C, a flow rate of 1 mL min^{-1}, and 5 mM H_2SO_4 as mobile phase. Proline and hyp were quantified using an identical HPLC system equipped with a diode array detector (VWR Hitachi L-2450) and an Inertsil ODS-3 column (4.6 x 150 mm, GL Sciences B.V., Eindhoven, Netherlands) as reported elsewhere (Theodosiou et al., 2015). Alternatively, a spectrophotometric method was used for hyp quantification (Falcioni et al., 2013).

Optical analysis of bacterial cells and cell size determination

Microscopic investigations and cell size determination were performed with a Zeiss Observer Z1 microscope equipped with a micro LED lamp as transmitted light illuminator and a high-resolution video camera Axiocam 503 mono (Carl Zeiss MicroImaging GmbH, Jena, Germany). Image processing and analysis were performed with Zen 2012 Blue Edition

Software (Carl Zeiss MicroImaging GmbH). For cell immobilization and imaging, low-melt agarose pads were used and prepared as described elsewhere (Young et al., 2011).

Results

Cellular physiology and biocatalytic response upon TCA cycle redesign

Either *sucA* or *sucC* was deleted together with *aceA* and *putA*, to determine the effect of TCA cycle engineering on host cell physiology and biocatalytic efficiency. Both triple mutant strains bearing either empty pET-24a(+) (no catalytic activity) or pET_p4h1of were incubated aerobically in glucose containing M9 minimal medium in presence or absence of L-proline.

The mutant strain lacking both SucA and P4H, that is 3Δ*sucA* (pET-24a(+)), was unable to grow in batch culture on glucose and proline in M9, which demonstrated the deleterious impact of impaired sucCoA synthesis for cultivation in minimal medium. The introduction of P4H restored growth ($\mu = 0.14\ h^{-1}$) and proline hydroxylation was exploited as a TCA cycle-restoring bypass at a rate of 0.49 mmol $g_{cdw}^{-1}\ h^{-1}$. Growth even was observed without external proline addition, albeit at a lower rate ($\mu = 0.10\ h^{-1}$) (**Fig. 2A**, **Table II**). Apparently, the endogenous proline hydroxylation rate (0.2 mmol $g_{cdw}^{-1}\ h^{-1}$) was sufficient to restore growth. Proline addition reduced the metabolic burden and enabled faster growth and glucose uptake (40% and 32% increase, respectively), as well as the acetate yield on glucose, which was reduced by 52%. However, also in the presence of proline hydroxylation, the decreased sucCoA pool and the absence of the glyoxylate shunt in the 3Δ*sucA* strain imposed a heavy stress as emphasized by the lower growth rate and final biomass concentration obtained as compared to the wildtype or the Δ*putA* single mutant (**Table II**).

Based on the fact that the growth of the 3Δ*sucA* mutant strain is coupled to proline hydroxylation, **Fig. 2B** shows the proof of principle for a selection method for the identification of active α-KG dependent hydroxylases or of new substrates for hydroxylation.

Only recombinant clones that produce active α-KG dependent dioxygenases as well as take up and hydroxylate the desired substrate (e.g., proline) will survive and grow on a substrate-containing minimal medium (selection for novel protein variants after directed evolution or novel enzymatic activities from gene banks). Alternatively, a recombinant clone producing the desired α-KG dependent dioxygenase can be used to identify novel substrates for this whole-cell biocatalyst, given that only the substrates that can be taken up and be hydroxylated will support host cell growth (selection to extend substrate spectrum).

The 3Δ*sucC* (pET-24a(+)) strain, contrary to 3Δ*sucA* (pET-24a(+)), was able to grow in minimal medium on glucose in the absence of P4H activity (**Table II**; **Supplemental Fig. S4**). In this case, the cells obtain sucCoA from α-KG via α-KG dehydrogenase and succinate via the activity of fumarate reductase. Upon P4H synthesis and independently of proline addition, both specific growth rate and biomass yield on glucose did not increase, but actually decreased. This indicates a metabolic burden imposed by heterologous P4H synthesis resulting in less energy and precursors available for biomass formation (Carneiro et al., 2013), as it has also been observed for the wildtype and the Δ*putA* strain (Theodosiou et al., 2015). However, it seems that, due to the disturbed TCA cycle, acetate was formed at a higher rate and was not assimilated when glucose got depleted (inactive glyoxylate shunt), resulting in a lower biomass yield on glucose. *SucC* deletion had no negative effect on the hyp formation rate, which was similar to that of the Δ*putA* strain. When proline was not extracellularly added, the hyp formation rate was dictated primarily by the intracellular proline formation rate and was at the same level as observed for the 3Δ*sucA* strain (0.18 and 0.20 mmol g_{cdw}^{-1} h^{-1}, respectively) (**Table II**).

In all cases, the growth rate of the 3Δ*sucA* strain was lower compared to the 3Δ*sucC*. Both strains were unable to assimilate acetate once glucose was depleted due to glyoxylate shunt deficiency (**Supplemental Fig. S5**). The greater severity of the *sucA* deletion and the higher

functional significance of SucA in the TCA cycle also become obvious from the longer lag phase (**Supplemental Fig. S5**) and the lower biomass yields on glucose (**Table II**). The highest metabolic stress was imposed on cells with growth dependent on the hydroxylation of intracellularly synthesized proline (**Table II**; 3Δ*sucA* (pET_p4h1of), -pro), i.e., fermentative hyp synthesis. In that case, the highest specific acetate formation rate and acetate yield on glucose were determined. The 3Δ*sucA* strain was chosen to further investigate the interplay between cellular metabolism and proline hydroxylation due to its biotransformation-dependent growth and also to identify possible strategies for improvement of the proline hydroxylation rate.

The putP transporter greatly enhances hyp synthesis rates in *E. coli* 3Δ*sucA*

The *putP* gene encoding a Na^+/L-proline transporter was co-expressed with *p4h1of* in order to examine whether enhanced proline uptake improves biocatalyst efficiency **(Fig. 3**; **Table III**). Expression of *p4h1of* and *putP* was induced with IPTG and arabinose, respectively.

The 3Δ*sucA* strain simultaneously consumed glucose and arabinose in all cases. It is well-documented that glucose is *E. coli*'s preferred carbon source repressing the uptake of other sugars (Deutscher, 2008). We assume that the observed co-metabolism resulted from the high arabinose concentration used which induced the genes responsible for its uptake (i.e., *araE* and *araFGH*) or from a not so tight catabolite repression by glucose. Arabinose altered the cellular carbon distribution significantly, even though it was not excessively consumed leaving more than half of the initial concentration at the end of the cultivation (**Table III**). In the presence of arabinose, specific acetate and hyp formation rates of the 3Δ*sucA* (pET_p4h1of) strain increased by 68 and 63%, respectively, whereas the glucose uptake rate decreased by 16%. We assume that arabinose was utilized via the pentose phosphate pathway for biomass formation, directing more glucose via glycolysis and the TCA cycle, thus increasing the formation of acetate and hyp. Remarkably, total conversion of proline was not

achieved within 60 h of cultivation in the presence of arabinose, even though both proline to support a functional TCA cycle and glucose to supply α-KG were still available (**Fig. 3A**). After 18-20 h, the cells entered a stationary phase and hyp synthesis continued at a lower rate up to 62% proline conversion after 60 h. This points at an inhibitory effect of acetate reached which is at the lower boundary of the reported growth-inhibiting concentrations (0.5 g L^{-1}) (Aristidou et al., 1994; Nakano et al., 1997).

In contrary, when putP was produced, quantitative conversion of proline was observed and the specific hyp synthesis rate increased by another 100% (**Fig. 3B**). In contrast, PutP had no beneficial effect on proline hydroxylation by Δ*putA* (**Table III**) and wildtype (**Supplemental Table 6**) strains. The almost full conversion of proline by the 3Δ*sucA* (pEB_p4h1of_putP) strain after 20 h and the consequent inability of the cells to shunt the TCA cycle additionally explain the residual amounts of glucose and arabinose. The improved biocatalytic performance of this strain correlated with increased glucose and decreased arabinose uptake rates, and lead to similar biomass levels compared to the 3Δ*sucA* (pET_p4h1of) strain. The fact that the yield of acetate on glucose was 20% lower at similar growth rate and final biomass titer indicates carbon redistribution in favor of hyp formation when PutP is overproduced. Increasing the substrate concentration (from 5 to 50 mM) did not enhance the hyp formation rate of the 3Δ*sucA* (pEB_p4h1of_putP) strain, indicating that, already at 5 mM, both the transporter and the P4H work at V_{max}, as can be concluded from their K_m values for proline of 3.3 µM and 1 mM, respectively (Falcioni et al., 2013) (**Table III**; **Supplemental Fig. 7**).

Deletion of *sucA* perturbs bacterial cell wall formation and cell size – medium supplementation partially restores morphology but not bacterial growth

SucCoA is not only an intermediate of the TCA cycle but also a precursor for biosynthesis of methionine, lysine, and diaminopimelate (DAP) for peptidoglycan formation (Patte, 1996;

Cabeen and Jacobs-Wagner, 2005) (**Supplemental Fig. S1**). Thus, growth of 3Δ*sucA* strains might be affected by limiting sucCoA availability. In order to address the role of sucCoA in growth physiology, the morphology of the 3Δ*sucA* (pET_p4h1of) strain and the effect of methionine, lysine, and DAP supplementation were investigated (**Table IV**).

Microscopic analysis and cell size determination confirmed the significant impact of the *sucA* deletion on cell morphology (**Fig. 4**). The average cell size was 27% lower compared to the wildtype (**Fig. 4B**), which also influenced the correlation between optical density (OD_{600}) and cell dry weight concentration (g_{cdw} L^{-1}) (**Supplemental Table S3**). When P4H-bearing cells were grown in M9 medium supplemented with glucose only, an OD_{600} of 1 corresponded to 0.339 and 0.211 g_{cdw} L^{-1} for the wildtype and the 3Δ*sucA* strain, respectively. Contrary to *sucA* deletion, the morphological effect of *sucC* deletion was negligible (**Fig. 4B**), being consistent with the fact that growth and biocatalytic performance were not severely affected.

The addition of 5 mM DAP neither improved growth rate nor biocatalytic efficiency of the 3Δ*sucA* (pET_p4h1of) strain, but lead to a 16% increase of the average cell size, which, therefore, was partly restored (**Fig. 4C**). In this case, DAP may have been taken up directly from the medium and incorporated into the cell wall, reducing the need for endogenous synthesis from sucCoA. Supplementation with L-lysine and L-methionine had no influence on the specific growth rate and only a minor impact on bacterial morphology (**Fig. 4C)**, but led to a significant increase in specific glucose uptake and hyp formation rates (by 75 and 125%, respectively), whereas biomass and acetate yields decreased. The degradation of methionine into sucCoA (Berg et al., 2002) may have relieved the broken TCA cycle, but did not support DAP synthesis to the same extent as external DAP addition. Lysine, being a ketogenic amino acid, can be degraded to acetyl-CoA, which may trigger TCA cycle flux and thus support hyp formation. Together, these effects obviously led to a largely increased glucose uptake rate and enabled the significant increase of glucose-derived hyp formation,

both in terms of rate and final titer. The addition of DAP into a lysine and methionine containing medium further increased the bacterial cell size (**Fig. 4C**), but reduced specific glucose uptake and hyp as well as acetate formation rates. All supplementation strategies enhanced bacterial cell wall formation by supplying DAP either directly or indirectly. However, the mutant strain did not completely recover the morphology of the wildtype strain.

Discussion

TCA cycle redesign for efficient whole-cell *trans*-4-hydroxy-L-proline synthesis

In *E. coli*, the *sucA* and *sucC* genes are located in the same operon *sucABCD*. The *sucA* gene encodes the E1 subunit of the *a*-KG dehydrogenase catalyzing the conversion of α-KG into sucCoA, while the *sucC* gene encodes the β-subunit of the sucCoA synthetase (Li et al., 2006). Literature reports are contradictory regarding the effect of *sucA* and *sucC* single gene deletions on growth, which seems to depend on both the genotypic differences among different *E. coli* strains and the applied engineering methodology (Yu et al., 2006). Furthermore, medium use is critical for the evaluation of knock out effects and cultivation on complex media can cause some bias. Yu et al. (2006) reported that *sucAB* and *sucCD* encode mutually essential enzymes, which can be deleted individually, causing prolonged lag phases, but not simultaneously. They investigated *E. coli* MG1655 in LB medium and combined deletions with conditional expression of the remaining *suc* operon (arabinose inducible Km^R-*araC*-P_{BAD} cassette). When cells were cultivated with 0.1% (w/v) arabinose, both Δ*sucAB* and Δ*sucCD* mutants grew at similar growth rates, which were 27-35% lower than that of the parental strain. Their findings differ from those of Integrated Genomics (http://www.integratedgenomics.com) reporting that the *sucAB* genes are essential but not *sucCD* and PEC database (http://www.shigen.nig.ac.jp/ecoli/pec) reporting that *sucABCD* are all nonessential. Li et al. (2006), working with the Keio collection strain *E. coli* BW25113 in minimal medium, observed that only *sucA* but not *sucC* deletion caused a longer lag phase

and a 20% growth rate decrease compared to the wildtype. The single *sucA* and *sucC* knockout mutants of *E. coli* BL21(DE3)(pLysS) generated in this work showed similar phenotypes as the Keio strains. Thereby, growth of the Δ*sucA* strain, which has been shown to be enabled by glyoxylate shunt activation (Li et al., 2006), was affected more dramatically (linear instead of exponential growth, data not shown).

We aimed to address the aforementioned glyoxylate shunt activation by constructing triple mutants of *E. coli* BL21(DE3)(pLysS) with either the *sucA* or *sucC* gene deleted together with the *aceA* and *putA* genes. The applied engineering strategy aimed not only at enhancing cosubstrate availability for P4H, but also at understanding the interplay between biotransformation and central carbon metabolism of host cells. Contrary to recently published results on *trans*-4-hydroxy-L-isoleucine synthesis involving 82% biotransformation yield, we avoided substrate, that is proline, catabolism via *putA* deletion enabling a yield of 100% (Theodosiou et al., 2015).

3Δ*sucC* cells devoid of P4H activity obviously have metabolic alternatives to overcome TCA cycle interruption. It is reported that inactivation of SucC does not activate the glyoxylate shunt, denoting that sucCoA is efficiently synthesized from α-KG and, more generally, that the enzyme inventory of Δ*sucC* strains is capable of sufficiently synthesizing all TCA cycle metabolites via oxidative and reverse action of the TCA cycle (Li et al., 2006). Mat-Jan et al. (1989) showed that SucC-deficient *E. coli* K12 cannot grow on acetate (inactive glyoxylate shunt) and α-KG (broken TCA cycle) but can grow on succinate, malate, and fumarate generating all the necessary TCA cycle intermediates. These findings are in agreement with our observation that deletion of both *aceA* and *sucC* did not significantly affect growth. Deletion of *sucC* together with *aceA* and *putA* in the catalytically active strain containing P4H lead to a phenotype that resembled that of the *putA* single mutant strain, except for a slightly decreased growth rate and enhanced acetate formation involving a reduced biomass

yield. These changes can be ascribed to a slower operation of the artificially closed TCA cycle. The Δ*putA* single knock out strain still is superior to this triple mutant, hydroxylating proline at a similar rate but with a lower glucose demand and less acetate formation.

Cells encountered the heaviest stress when the *sucA* gene was knocked out, as obvious from their physiological and morphological responses. It is reported that, upon *sucA* deletion, the glyoxylate shunt is activated to efficiently provide oxaloacetate and sucCoA for biomass synthesis (Li et al., 2006). In the same report, flux analysis results indicated that *sucA* deletion also activated the pentose phosphate pathway and anaplerotic reactions such as phosphoenolpyruvate (PEP) carboxylase, PEP carboxykinase, and malate dehydrogenase, while the fluxes through glycolysis and the TCA cycle were downregulated. In glyoxylate shunt-deficient *E. coli*, it was shown that PEP carboxylation constitutes the only remaining anaplerotic route for oxaloacetate replenishment (Sauer and Eikmanns, 2005). Upon combined SucA and glyoxylate shunt deletion, cells became unable to grow in minimal medium. SucCoA synthesis relies on the conversion of succinate to sucCoA and other minor pathways like amino (methionine, isoleucine, threonine, and valine) or fatty acid degradation, rendering it the rate-limiting step in microbial growth. When the heterologous *p4h1of* gene is expressed, proline hydroxylation serves as an alternative pathway for succinate supply, apparently taking over the functional role of the glyoxylate shunt pathway to sustain growth. Survival and growth of the 3Δ*sucA* mutant is coupled to product formation and key limitations are imposed by the host physiology and also the *in vivo* kinetic parameters of the employed proline hydroxylase. Under the aerobic conditions applied, possible limitations of product formation and growth of the 3Δ*sucA* mutant include proline uptake and α-KG supply that is TCA cycle flux. The relief of such limitations can furthermore be expected to reduce acetate formation, which would give the additional benefit of reducing possible acetate-related toxic effects on the host strain.

Besides metabolic and regulatory networks, transport reactions are also essential for whole-cell biocatalysis. Membrane transporters have been highlighted as excellent targets for strain improvement, though yet underutilized (Julsing et al., 2012; Cornelissen et al., 2013; Kell et al., 2015; Ladkau at al., 2016). The Na^+/proline permease PutP employed in this work is an integral cytoplasmic membrane protein that catalyzes the coupled translocation of proline and Na^+ or Li^+ ions (Quick et al., 1996). PutP introduction into the P4H containing 3Δ*sucA* strain doubled the specific proline hydroxylation rate, slightly increased the growth rate, and reduced the acetate formation rate as expected for the relieve of P4H limitation (**Table III**). In contrast, PutP had, beside a slightly increased μ, no beneficial effect on Δ*putA* and wildtype (**Supplemental Table S6**) strains containing P4H. This indicates that proline hydroxylation was limited by α-KG availability, which obviously was relieved when the *sucA* gene was deleted and α-KG could not be utilized via the TCA cycle anymore. Increasing the extracellular proline concentration could not substantially enhance hyp formation rates, probably due to low K_m values for proline of both PutP and P4H. In this case, engineering strategies aiming at improving the *in vivo* catalytic properties of both transporter and hydroxylase may be promising.

Beside the promising catalytic properties of the 3Δ*sucA* mutant in the presence of PutP, this strain can be considered advantageous as it allows antibiotic-free bioprocessing due to its biotransformation-dependent growth. This is of great importance considering the efforts of the biotechnology industry to eliminate antibiotics from production processes and provide final products free from antibiotics.

The 3Δ*sucA* strain also was demonstrated to be suitable for the selection for active α-KG dependent oxygenation (**Fig 2B**). Selection can either target the enzyme, supplementing minimal agar with the substrate of interest, or the substrate scope, testing different substrates with a strain containing a specific α-KG dependent dioxygenase. Thereby, selection methods

can serve as powerful tools for the screening of respective enzyme libraries derived from metagenomics, strain collections, or random mutagenesis. More specifically, an L-proline-4-hydroxylase library generated via random mutagenesis can be screened for variants with improved catalytic properties. Regarding the substrate spectrum, unnatural amino acids would be very attractive targets to be tested, in order to enable the enantioselective synthesis of novel chiral amino acid derivatives.

Impact of morphological changes on whole-cell physiology and biocatalytic efficiency

In bacteria, cell morphology affects many physiological processes, such as cell division, motility, nutrient/substrate uptake, and biofilm formation. Elucidating the factors activating mechanisms for cell-shape maintenance and cell-size determination is important for understanding and manipulating bacterial physiology (Tropini et al., 2014). By deleting the main reaction supplying cells with sucCoA, we hindered the synthesis of diaminopimelate (DAP), an essential constituent of the cell wall, and thereby perturbed cell wall formation. Cells responded to the deletion of *sucA* by decreasing their average size by 27% compared to the wildtype. This morphological alteration was found to strongly influence the correlation factor between OD_{600} and cell dry weight concentration (g_{cdw} L^{-1}). Gene deletions can thus heavily change optical properties of microbial cells, highlighting that correlation factors should be determined afresh for each individual (engineered) strain.

Different medium supplementation strategies were tested to investigate whether the wiltype cell morphology can be restored. L-lysine and L-methionine were chosen due to their interconnection with the pool of sucCoA, which is involved in their biosynthesis. DAP was chosen due to its role in cell wall synthesis. It can be stated based on the average cell size increase upon DAP supplementation that cells could directly utilize it for peptidoglycan synthesis. However, the metabolic burden imposed by the decreased sucCoA pool was not relieved and glucose-derived hyp formation was not enhanced. Lysine and methionine supply

restored cell morphology only to a minor extent, but clearly facilitated TCA cycle operation and thus hyp formation, but not growth, probably due to the higher carbon loss via acetate formation. The supply of lysine and methionine via the culture medium also made their synthesis expendable as they could be used directly for protein synthesis. In that case, the highest fermentative hyp formation was observed owing to the rather high metabolic flux towards α-KG. This carbon withdrawal from the TCA cycle for P4H catalysis may be responsible for the lower biomass yields. Together with the effect of *putP* overexpression, the high fermentative hyp formation rate of the triple mutant under all supplementation conditions stresses the beneficial effect of inactivating the α-KG dehydrogenase and directing α-KG towards P4H catalysis. Fermentative hyp formation already was pronounced (2.5 fold higher compared to the wildtype) when medium containing only glucose was used.

Conclusions

In this work, we provided insight into α-KG dependent whole-cell biocatalysis by recruiting TCA cycle engineering and overexpression of a substrate transporter. The TCA cycle of *E. coli* BL21(DE3)(pLysS) bearing an α-KG dependent proline hydroxylase was disrupted by either deleting the genes *sucA* or *sucC* and by inactivating the glyoxylate shunt pathway. The TCA cycle displayed different functional structures upon engineering. The deletion of *sucC* in combination with *aceA* led to increased acetate formation but did not impair growth, whereas the deletion of *sucA* and *aceA* only allowed growth upon TCA re-cyclization via P4H catalyzed proline hydroxylation. The latter further effected a decreased average cell size. Most importantly, the *sucA* deletion relieved the competition for α-KG between the α-KG dehydrogenase and proline hydroxylase so that the overexpression of *putP* enabled a significantly increased specific proline hydroxylation rate in the Δ*sucA*Δ*aceA*Δ*putA* strain. Such a PutP effect could not be achieved in the Δ*putA* strain that still has an active α-KG dehydrogenase, which obviously lead to a P4H activity limited by α-KG instead of proline

availability. These findings provide strong evidence that the competition for α-KG between the TCA cycle and the P4H enzyme determines the proline hydroxylation activity of the whole-cell biocatalyst and constitutes a main target for optimization. Such optimization was successfully achieved by combining *sucA*, *aceA*, and *putA* deletions with *putP* overexpression. Finally, this work highlights the potential of Δ*sucA*Δ*aceA* mutants as a powerful selection tools for novel α-KG dependent dioxygenases with improved biocatalytic activity *in vivo*.

Acknowledgments

This work was financially supported by the EU-FP7 Oxygreen project (FP7 EU grant number 212281) and the Mercator Research Center Ruhr (MERCUR, Pr-2013-0010). We gratefully acknowledge Christian Dusny and Ron Stauder for their help in microscopy and agarose pad preparation and Kai Sai for experimental assistance.

The authors declare no conflict of interest.

References

Aristidou AA, San KY, Bennett GN. 1994. Modification of central metabolic pathway in *Escherichia coli* to reduce acetate expression of the *Bacillus subtilis* acetolactate synthase gene. Biotechnol Bioeng 44:944-951.

Berg JM, Tymoczko JL, Stryer, L. 2002. Biochemistry, 5th Edition, W.H. Freeman & Co., New York.

Blank LM, Ebert BE, Bühler B, Schmid A. 2008. Metabolic capacity estimation of *Escherichia coli* as a platform for redox biocatalysis: constraint-based modeling and experimental verification. Biotechnol Bioeng 100:1050-1065.

Blank LM, Ebert BE, Bühler K, Buhler B. 2010. Redox biocatalysis and metabolism: Molecular mechanisms and metabolic network analysis. Antioxid Redox Signal 13:349-394.

Bühler B, Bollhalder I, Hauer B, Witholt B, Schmid A. 2003. Use of the two-liquid phase concept to exploit kinetically controlled multistep biocatalysis. Biotechnol Bioeng 81:683-694.

Cabeen MT and Jacobs-Wagner C. 2005. Bacterial cell shape. Nat Rev Microbiol 3:601-610.

Carneiro S, Ferreira EC, Rocha I. 2013. Metabolic responses to recombinant bioprocesses in *Escherichia coli*. J Biotech 164:396-408.

Cornelissen S, Julsing MK, Volmer J, Riechert O, Schmid A, Bühler B. 2013. Whole-cell-based CYP153A6-catalyzed (S)-limonene hydroxylation efficiency depends on host background and profits from monoterpene uptake via AlkL. Biotechnol Bioeng 110:1282-1292.

Cozzone AJ and El-Mansi M. 2005. Control of isocitrate dehydrogenase catalytic activity by protein phosphorylation in *Escherichia coli*. J. Mol. Microbiol Biotechnol 9:132-146.

Datsenko KA and Wanner BL. 2000. One-step inactivation of chromosomal genes in *Escherichia coli* K-1 using PCR products. Proc Natl Acad Sci USA 97:6640-6645.

Deutscher J. 2008. The mechanisms of carbon catabolite repression in bacteria. Curr Opin Microbiol 11:87-93.

Falcioni F, Blank LM, Frick O, Karau A, Bühler B, Schmid A. 2013. Proline availability regulates proline-4-hydroxylase synthesis and substrate uptake in proline-hydroxylating recombinant *Escherichia coli*. Appl Environ Microbiol 79:3091-3100.

Gibson DG, Young L, Chuang RY, Venter JC, Hutchison CA 3rd, Smith HO. 2009. Enzymatic assembly of DNA molecules up to several hundred kilobases. Nat Methods 6:343-345.

Hara R and Kino K. 2009. Characterization of novel 2-oxoglutarate dependent dioxygenases converting L-proline to *cis*-4-hydroxy-l-proline. Biochem Biophys Res Commun 379:882-886.

Hausinger RP. 2004. Fe(II)/alpha-ketoglutarate-dependent hydroxylases and related enzymes. Crit Rev Biochem Mol Biol 39:21-68.

Julsing MK, Schrewe M, Cornelissen S, Hermann I, Schmid A, Bühler B. 2012. The outer membrane protein AlkL boosts biocatalytic oxyfunctionalization of hydrophobic substrates in *E. coli*. Appl Environ Microbiol 78:5724-5733.

Kell DB, Swainston N, Pir P, Oliver SG. 2015. Membrane transporter engineering in industrial biotechnology and whole cell biocatalysis. Trends Biotechnol 33:237-246.

Ladkau N, Aßmann M, Schrewe M, Julsing MK, Schmid A, Bühler B. 2016. Efficient production of the Nylon 12 monomer ω-aminododecanoic acid methyl ester from renewable dodecanoic acid methyl ester with engineered *Escherichia coli*. Metab Eng 36:1-9.

Li M, Ho PY, Yao S, Shimizu K. 2006. Effect of *sucA* or *sucC* gene knockout on the metabolism in *Escherichia coli* based on gene expressions, enzyme activities, intracellular metabolite concentrations and metabolic fluxes by ^{13}C-labeling experiments. Biochem Eng J 30:286-296.

Mat-Jan F, Williams CR, Clark DP. 1989. Anaerobic growth defects resulting from gene fusions affecting succinyl-CoA synthetase in *Escherichia coli* K12. Mo Gen Genet 215:276-280.

Moffatt BA, Studier FW. 1987. T7 lysozyme inhibits transcription by T7 RNA-polymerase. Cell 49:221-227.

Nakano K, Rischke M, Sato S, Märkl H. 1997. Influence of acetic acid on the growth of *Escherichia co*li K12 during high-cell-density cultivation in a dialysis reactor. Appl Microbiol Biotechnol 48:597-601.

Patte JC. 1996. Biosynthesis of threonine and lysine. In: *Escherichia coli* and *Salmonella typhimurium* (Neidhardt, F.C., Ed.), American Society for Microbiology, Washington, DC. Vol. 2, p 528-541.

Quick M, Tebbe S, Jung H. 1996. Ser57 in the Na+/proline permease of *Escherichia coli* is critical for high-affinity proline uptake. Eur. J. Biochem. 239:732-736.

Sambrook J and Russell D. 2001. Molecular Cloning: a Laboratory Manual, 3rd edn. Cold Spring Harbor Laboratory, Cold Spring Harbor.

Sauer U and Eikmanns BJ. 2005. The PEP-pyruvate-oxaloacetate node as the switch point for carbon flux distribution in bacteria. Fems Microbiol Rev 29:765-794.

Schrewe M, Julsing MK, Buhler B, Schmid A. 2013. Whole-cell biocatalysis for selective and productive C-O functional group introduction and modification. Chem Soc Rev 42:6346-6377.

Smirnov SV, Kodera T, Samsonova NN, Kotlyarova VA, Rushkevich NY, Kivero AD, Sokolov PM, Hibi M, Ogawa J, Shimizu S. 2010. Metabolic engineering of *Escherichia coli* to produce (2S, 3R, 4S)-4-hydroxyisoleucine. Appl Microbiol Biotechnol 88:719-726.

Theodosiou E, Frick O, Bühler B, Schmid A. 2015. Metabolic network capacity of *Escherichia coli* for Krebs cycle-dependent proline hydroxylation. Microb Cell Fact 14:108.

Tropini C, Lee TK, Hsin J, Desmarais SM, Ursell T, Monds RD, Huang KC. 2014. Principles of bacterial cell-size determination revealed by cell-wall synthesis perturbations. Cell Rep 9:1520-1527.

Young JW, Locke JC, Altinok A, Rosenfeld N, Bacarian T, Swain PS, Mjolsness E, Elowitz MB. 2011. Measuring single-cell gene expression dynamics in bacteria using fluorescence time-lapse microscopy. Nat Protoc 7:80-88.

Yu BJ, Sung BH, Lee JY, Son SH, Kim MS, Kim SC. 2006. *sucAB* and *sucCD* are mutually essential genes in *Escherichia coli*. FEMS Microbiol Lett 254:245-250.

Figure legends

Figure 1. Hydroxylation of L-proline catalyzed by L-proline-4-hydroxylase (P4H) using recombinant *E. coli* cells and its interconnection with host central carbon metabolism. Targeted genes for TCA cycle redesign are highlighted in red.

Figure 2. Coupling bacterial survival and growth to P4H activity. **A**) Growth of the *E. coli* 3Δ*sucA* strain bearing either pET-24a(+) (pET) (closed symbols) or pET_p4h1of (open symbols) in M9 medium supplemented with glucose (Glc) only or glucose and proline (Pro) at 30 °C. **B**) Selection method using the 3Δ*sucA* strain to identify active α-KG dependent hydroxylases. Antibiotic-free M9 plates were supplemented with glucose only (left plate) or glucose and proline (right plate). **I**) *E. coli* wt (pET_p4h1of), **II**) *E. coli* 3Δ*sucC* (pET_p4h1of), **III**) *E. coli* 3Δ*sucA* (pET-24a(+)), and **IV**) *E. coli* 3Δ*sucA* (pET_p4h1of).

Figure 3. Effect of overexpressing the proline transporter gene *putP* on microbial physiology and hyp synthesis in a P4H containing 3Δ*suc*A mutant. Panels **A** and **B** show biomass formation, glucose consumption, arabinose consumption, acetate formation, and hyp synthesis during batch cultivation at 30 °C of *E. coli* 3Δ*sucA* (pET_p4h1of) and *E. coli* 3Δ*sucA* (pEB_p4h1of_putP), respectively, in M9 medium supplemented with 5 g L^{-1} glucose, 2 g L^{-1} arabinose, 5 mM L-proline, and 0.2 mM IPTG (see also **Table III**).

Figure 4. Morphological comparison of pET_p4h1of containing *E. coli* wt, 3Δ*sucC*, and 3Δ*sucA*. **A**) Microscopic analysis. **B**) Cell size distribution upon *sucC* and *sucA* deletion. **C**) Cell size distribution of 3Δ*sucA* upon medium supplementation. Cells were grown at 30 °C in 5 g L^{-1} glucose containing M9 medium, optionally supplemented with 5 mM diaminopimelate (DAP), L-lysine (Lys), and/or L-methionine (Meth), and harvested in the exponential phase. n, number of analyzed individual cells; L_A, average cell length; Cv, coefficient of variation (%).

Table I. Bacterial strains and plasmids used in this study.

Strains and Plasmids (Abbreviation)	Description	Source
E. coli BL21(DE3)(pLysS) (wt)	F^{-} *ompT hsdS*$_B$(r_B^- m_B^-) *gal dcm* (DE3) p*LysS* (Cm^R)	Invitrogen™ USA
E. coli BL21Δ*sucA*Δ*aceA*Δ*putA*(DE3)(pLysS) (3Δ*sucA*)	Deletion of *sucA*, *aceA*, and *putA* encoding *α*-KG dehydrogenase E1 subunit, isocitrate lyase (ICL), and proline dehydrogenase (PutA), respectively	This study
E. coli BL21Δ*sucC*Δ*aceA*Δ*putA*(DE3)(pLysS) (3Δ*sucC*)	Deletion of *sucC*, *aceA*, and *putA* encoding succinyl-CoA synthetase *β* subunit, isocitrate lyase (ICL), and proline dehydrogenase (PutA), respectively	This study
pLysS	Carries the gene for T7 phage lysozyme, an inhibitor for T7 polymerase, Cm^R	Moffatt and Studier, 1987
pET-24a(+)	High copy number vector, ColE1 ori, T7lac promoter, Km^R	Novagen
pET_p4h1of	pET-24a(+) containing codon-optimized *p4h1of* gene (*Dactylosporangium* sp), Km^R	Falcioni et al., 2013
pEB_p4h1of_putP	IPTG inducible T7 promotor, arabinose inducible BAD promotor, *p4h1of*, *putP*, Km^R	This study
pRedET	Contains *recE* and *recT* for homologous recombination. Temperature and L-arabinose inducible, Amp^R or Tet^R	Gene Bridges GmbH, Heidelberg, Germany
pCP20	Contains a flippase gene responsible for cassette disruption, Amp^R and Cm^R	Datsenko and Wanner, 2000

Table II. Physiological parameters of recombinant *E. coli* BL21(DE3)(pLysS) triple mutant strains in absence (pET-24a(+)) or presence of P4H activity (pET_p4h1of) and L-proline.

	***wt (pET_p4h1of)**	***Δ*putA* (pET_p4h1of)**	**3Δ*sucA* (pET-24a(+))**	**3Δ*sucA* (pET_p4h1of)**		**3Δ*sucC* (pET-24a(+))**		**3Δ*sucC* (pET_p4h1of)**	
	+Pro	+Pro	-Pro/+Pro	-Pro	+Pro	-Pro	+Pro	-Pro	+Pro
μ (h^{-1})	0.33 ± 0.01	0.32 ± 0.01	no growth	0.10 ± 0.01	0.14 ± 0.01	0.39 ± 0.01	0.40 ± 0.01	0.26 ± 0.01	0.28 ± 0.01
Final biomass (g_{cdw} L^{-1})	1.80 ± 0.10	1.50 ± 0.10	NA	0.63 ± 0.02	0.81 ± 0.01	1.57 ± 0.07	1.62 ± 0.02	1.52 ± 0.03	1.62 ± 0.03
r_{glc} (mmol g_{cdw}^{-1} h^{-1})	-4.40 ± 0.30	-3.90 ± 0.10	NA	-3.96 ± 0.07	-5.21 ± 0.04	-6.17 ± 0.05	-6.06 ± 0.01	-5.05 ± 0.24	-4.92 ± 0.18
r_{ace} (mmol g_{cdw}^{-1} h^{-1})	1.24 ± 0.10	0.93 ± 0.10	NA	2.49 ± 0.11	1.56 ± 0.06	1.98 ± 0.11	1.90 ± 0.15	1.83 ± 0.1	1.59 ± 0.18
r_{pro} (mmol g_{cdw}^{-1} h^{-1})	-0.68 ± 0.01	-0.75 ± 0.01	NA	NA	-0.49 ± 0.01	NA	NA	NA	-0.74 ± 0.08
r_{hyp} (mmol g_{cdw}^{-1} h^{-1})	0.37 ± 0.01	0.75 ± 0.01	NA	0.20 ± 0.02	0.49 ± 0.01	NA	NA	0.18 ± 0.01	0.77 ± 0.09
$Y_{x/s}$ (g_{cdw} g_{glc}^{-1})	0.42 ± 0.03	0.45 ± 0.01	NA	0.14 ± 0.01	0.15± 0.01	0.35 ± 0.01	0.37 ± 0.01	0.29 ± 0.01	0.32 ± 0.01
$Y_{ace/s}$ (mol_{ace} mol_{glc}^{-1})	0.28 ± 0.01	0.24 ± 0.03	NA	0.63 ± 0.01	0.30 ± 0.01	0.32 ± 0.02	0.31 ± 0.02	0.36 ± 0.01	0.32 ± 0.03
$Y_{hyp/s}$ (mol_{hyp} mol_{glc}^{-1})	0.08 ± 0.01	0.19 ± 0.01	NA	0.05 ± 0.01	0.09 ± 0.01	NA	NA	0.04 ± 0.01	0.16 ± 0.01
$Y_{hyp/pro}$ (mol_{hyp} mol_{pro}^{-1})	0.55 ± 0.01	1.00 ± 0.01	NA	NA	1.00 ± 0.01	NA	NA	NA	1.00 ± 0.01
C_{ace} (g L^{-1})[(1)]	0.26 ± 0.01	0.22 ± 0.01	NA	1.44 ± 0.02	0.91 ± 0.01	0.53 ± 0.03	0.54 ± 0.01	0.60 ± 0.01	0.54 ± 0.03
C_{hyp} (mM)[(1)]	3.0 ± 0.1	5.0 ± 0.1	NA	1.4 ± 0.1	4.8 ± 0.1	NA	NA	1.3 ± 0.1	4.8 ± 0.2
Specific P4H activity (U g_{cdw}^{-1})	6.1 ± 0.2	12.6 ± 0.1	NA	3.4 ± 0.3	8.1 ± 0.1	NA	NA	2.95 ± 0.14	12.1 ± 1.5

Strains were grown aerobically at 30 °C in M9 medium containing 5 g L^{-1} glucose in the absence or presence of 5 mM L-proline. μ, specific growth rate; *r*, specific rate for substrate uptake (negative values) or product formation; pro, proline; glc, glucose; ace, acetate; hyp, *trans*-4-hydroxy-L-proline; $Y_{x/s}$, biomass yield on glucose; $Y_{ace/s}$, $Y_{hyp/s}$, and $Y_{hyp/pro}$, yield coefficients for products (yields are calculated during the exponential phase); NA, not applicable; 1 U = 1 μmol of product formed per min; [(1)] final acetate and hyp titers at the end of cultivation. *Results from Theodosiou et al. (2015).

Table III. Effect of PutP on growth physiology and hyp synthesis by P4H containing single mutant Δ*put*A and triple mutant 3Δ*suc*A.

	Δ*putA* (pET_p4h1of)	**Δ*putA* (pEB_p4h1of_putP)**	**3Δ*sucA* (pET_p4h1of)**		**3Δ*sucA* (pEB_p4h1of_putP)**		
	5mM Pro; +ara	**5mM Pro; +ara**	**5mM Pro; -ara**	**5mM Pro; +ara**	**5mM Pro; +ara**	**25mM Pro; +ara**	**50mM Pro; +ara**
μ (h^{-1})	0.34 ± 0.01	0.39 ± 0.01	0.14 ± 0.01	0.16 ± 0.01	0.18± 0.01	0.19 ± 0.01	0.19 ± 0.01
Final biomass (g_{cdw} L^{-1})	1.51 ± 0.06	1.08 ± 0.03	0.81 ± 0.01	0.62 ± 0.01	0.69 ± 0.02	0.72 ± 0.01	0.80 ± 0.06
r_{glc} (mmol g_{cdw}^{-1} h^{-1})	-4.56 ± 0.14	-4.82 ± 0.04	-5.21 ± 0.04	-4.40 ± 0.08	-4.98 ± 0.08	-5.07 ± 0.05	-4.82 ± 0.12
r_{ara} (mmol g_{cdw}^{-1} h^{-1})	-3.10 ± 0.06	-2.26 ± 0.11	NA	-1.33 ± 0.03	-0.53 ± 0.01	-0.59 ± 0.01	-0.61 ± 0.03
r_{ace} (mmol g_{cdw}^{-1} h^{-1})	2.78 ± 0.34	2.81 ± 0.17	1.56 ± 0.06	2.62 ± 0.03	2.38 ± 0.04	2.25 ± 0.02	1.30 ± 0.04
r_{hyp} (mmol g_{cdw}^{-1} h^{-1})	0.65 ± 0.06	0.57 ± 0.04	0.49 ± 0.01	0.80 ± 0.01	1.72 ± 0.01	1.70 ± 0.02	1.78 ± 0.01
$Y_{x/s}$ (g_{cdw} g_{glc}^{-1})	0.42 ± 0.01	0.45 ± 0.01	0.15± 0.01	0.21 ± 0.01	0.20 ± 0.01	0.21 ± 0.01	0.21 ± 0.01
$Y_{ace/s}$ (mol_{acet} mol_{glc}^{-1})	0.61 ± 0.06	0.58 ± 0.03	0.30 ± 0.01	0.60 ± 0.01	0.48 ± 0.02	0.44 ± 0.01	0.27 ± 0.02
$Y_{hyp/s}$ (mol_{hyp} mol_{glc}^{-1})	0.14 ± 0.01	0.12 ± 0.01	0.09 ± 0.01	0.182 ± 0.01	0.35 ± 0.01	0.33 ± 0.02	0.37 ± 0.01
C_{glc} (g L^{-1})[(1)]	0.54 ± 0.02	0.55 ± 0.05	0	1.54 ± 0.01	0.92 ± 0.01	0.51 ± 0.02	0.53 ± 0.01
C_{ara} (g L^{-1})[(1)]	0	0	NA	1.45 ± 0.02	1.67 ± 0.01	1.54 ± 0.06	1.46 ± 0.01
C_{ace} (g L^{-1})[(1)]	1.58 ± 0.12	0.96 ± 0.14	0.91 ± 0.01	0.83 ± 0.02	1.03 ± 0.01	0.88 ± 0.02	0.46 ± 0.02
C_{hyp} (mM) [(1)]	4.7 ± 0.1	3.9 ± 0.3	4.8 ± 0.1	3.1 ± 0.1	5.2 ± 0.1	7.5 ± 0.3	8.6 ± 0.1
Specific P4H activity (U g_{cdw}^{-1})	10.8 ± 1.0	9.6 ± 0.6	8.1 ± 0.1	12.7 ± 0.1	27.3 ± 0.3	27.6 ± 0.1	28.6 ± 0.4

E. coli Δ*putA* and 3Δ*sucA* strains were grown aerobically at 30 °C in M9 medium containing 5 g L^{-1} glucose, 2 g L^{-1} arabinose, and 0.2 mM IPTG in the absence or presence of 5, 25, or 50 mM proline. μ, specific growth rate; r, specific rate for substrate uptake (negative values) or product formation; glc, glucose; ara, arabinose; ace, acetate; hyp, *trans*-4-hydroxy-L-proline; $Y_{x/s}$, biomass yield on glucose; $Y_{ace/s}$ and $Y_{hyp/s}$, yield coefficients for products (yields are calculated during the exponential phase); NA, not applicable; 1 U = 1 μmol of product formed per min; [(1)] final glucose, arabinose, acetate, and hyp titers at the end of cultivation.

Table IV. Growth physiology of *E. coli* 3Δ*sucA* (pET_p4h1of) upon supplementation with DAP, L-lysine, and/or L-methionine.

	wt (pET_p4h1of)	**3Δ*sucA* (pET_p4h1of)**			
	Glc	**Glc**	**DAP**	**Lys+Meth**	**DAP+Lys+Meth**
μ (h^{-1})	0.32 ± 0.02	0.10 ± 0.01	0.09 ± 0.01	0.10 ± 0.01	0.11 ± 0.01
Final biomass (g_{cdw} L^{-1})	1.40 ± 0.10	0.63 ± 0.02	0.40 ± 0.01	0.47 ± 0.01	0.58 ± 0.02
r_{glc} (mmol g_{cdw}^{-1} h^{-1})	-4.80 ± 0.30	-3.96 ± 0.07	-3.66 ± 0.24	-6.93 ± 0.33	-5.87 ± 0.19
r_{ace} (mmol g_{cdw}^{-1} h^{-1})	0.92 ± 0.10	2.49 ± 0.11	2.13 ± 0.09	2.92 ± 0.24	2.04 ± 0.01
r_{hyp} (mmol g_{cdw}^{-1} h^{-1})	0.09 ± 0.01	0.20 ± 0.02	0.15 ± 0.03	0.45 ± 0.06	0.28 ± 0.02
Yx/s (g_{cdw} g_{glc}^{-1})	0.39 ± 0.02	0.14 ± 0.01	0.13 ± 0.01	0.08 ± 0.01	0.10 ± 0.01
$Y_{ace/s}$ (mol_{ace} mol_{glc}^{-1})	0.19 ± 0.01	0.63 ± 0.01	0.59 ± 0.06	0.42 ± 0.01	0.35 ± 0.01
$Y_{hyp/s}$ (mol_{hyp} mol_{glc}^{-1})	0.02 ± 0.01	0.05 ± 0.01	0.04 ±0.01	0.07 ± 0.01	0.05 ± 0.01
C_{ace} (g L^{-1})	0.16 ± 0.03[(1)]	1.44 ± 0.02[(2)]	1.02 ± 0.07[(2)]	0.73 ± 0.06[(2)]	0.72 ± 0.02[(2)]
C_{hyp} (mM) [(3)]	0.34 ± 0.01	1.42 ± 0.01	0.86 ± 0.02	1.66 ± 0.06	1.57 ± 0.06
Specific P4H activity (U g_{cdw}^{-1})	1.35 ± 0.02	3.36 ± 0.28	2.53 ± 0.07	7.50 ± 0.97	4.87 ± 0.38

Cells were grown aerobically at 30 °C in M9 medium containing 5 g L^{-1} glucose in the presence or absence of 5 mM diaminopimelate (DAP), L-lysine (Lys), and/or L-methionine (Meth). μ, specific growth rate; r, specific rate for substrate uptake (negative values) or product formation; pro, proline; ace, acetate; hyp, *trans*-4-hydroxy-L-proline; $Y_{x/s}$, biomass yield on glucose; $Y_{ace/s}$ and $Y_{hyp/s}$, yield coefficients for products (yields are calculated during the exponential phase); NA, not applicable; 1 U = 1 μmol of product formed per min; [(1)] final acetate titer upon glucose depletion; [(2)] final acetate titer at the end of cultivation; [(3)] final hyp titer at the end of cultivation.

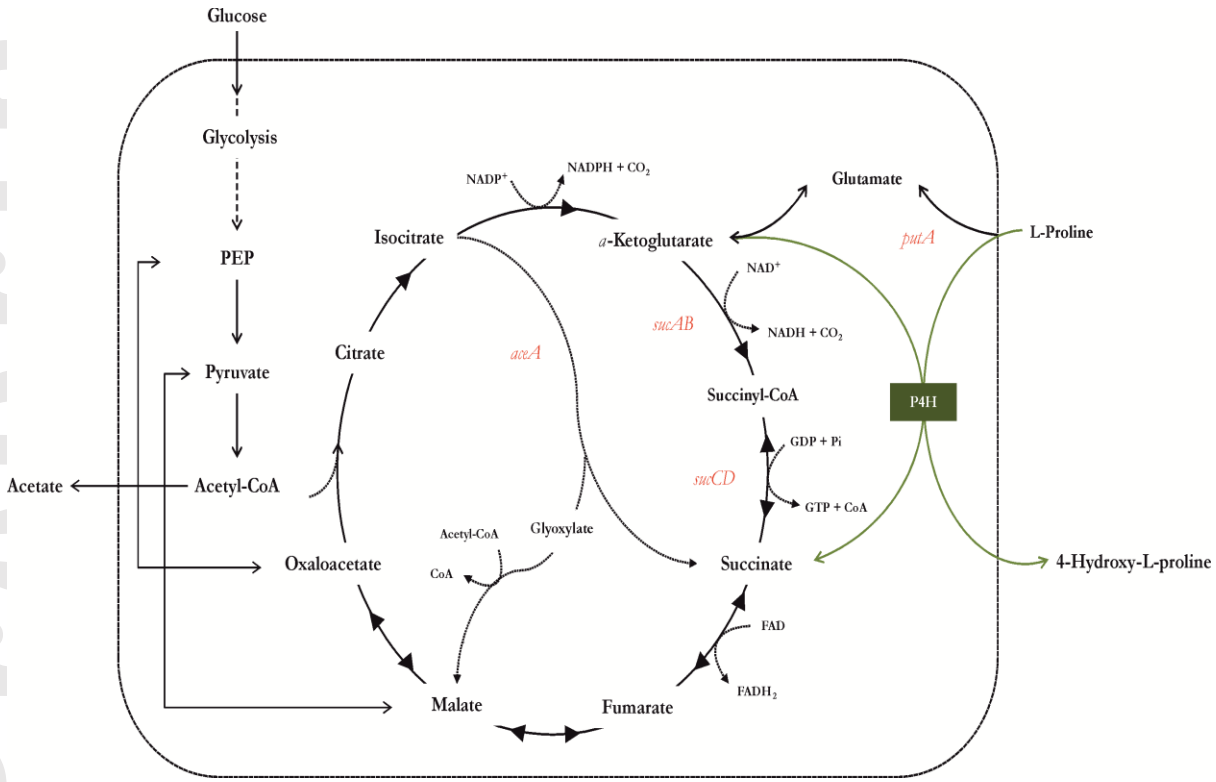

Figure 1

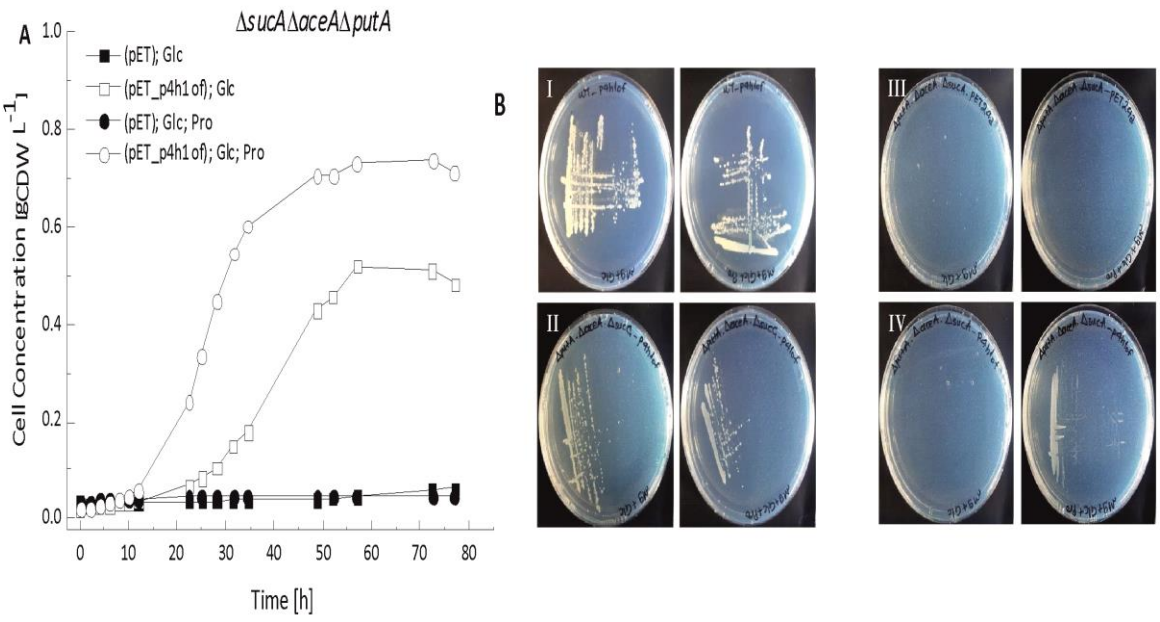

Figure 2

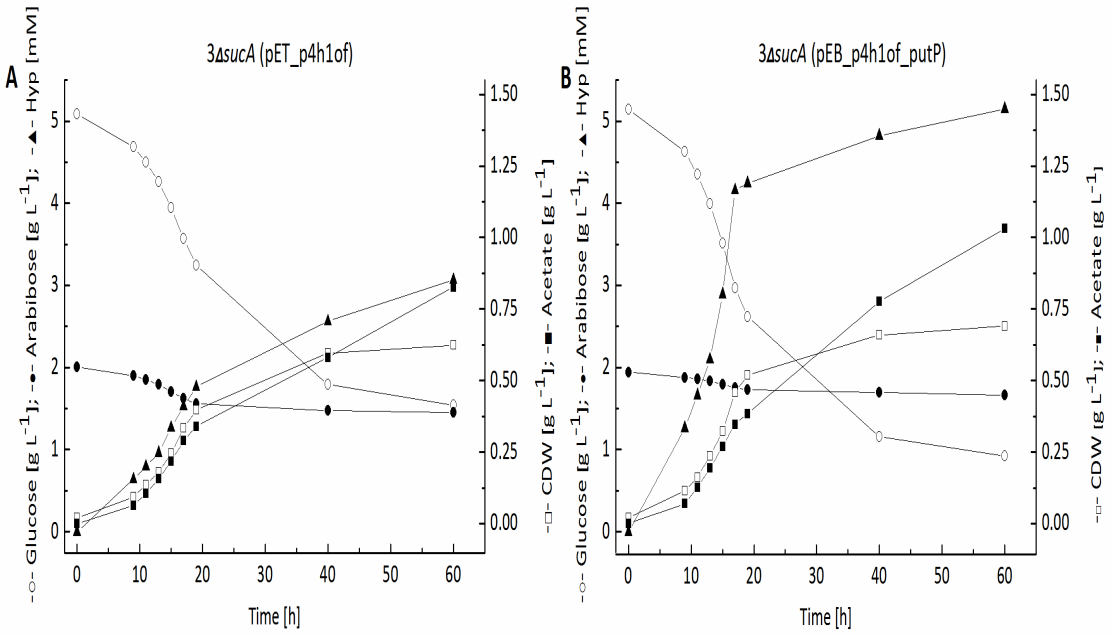

Figure 3

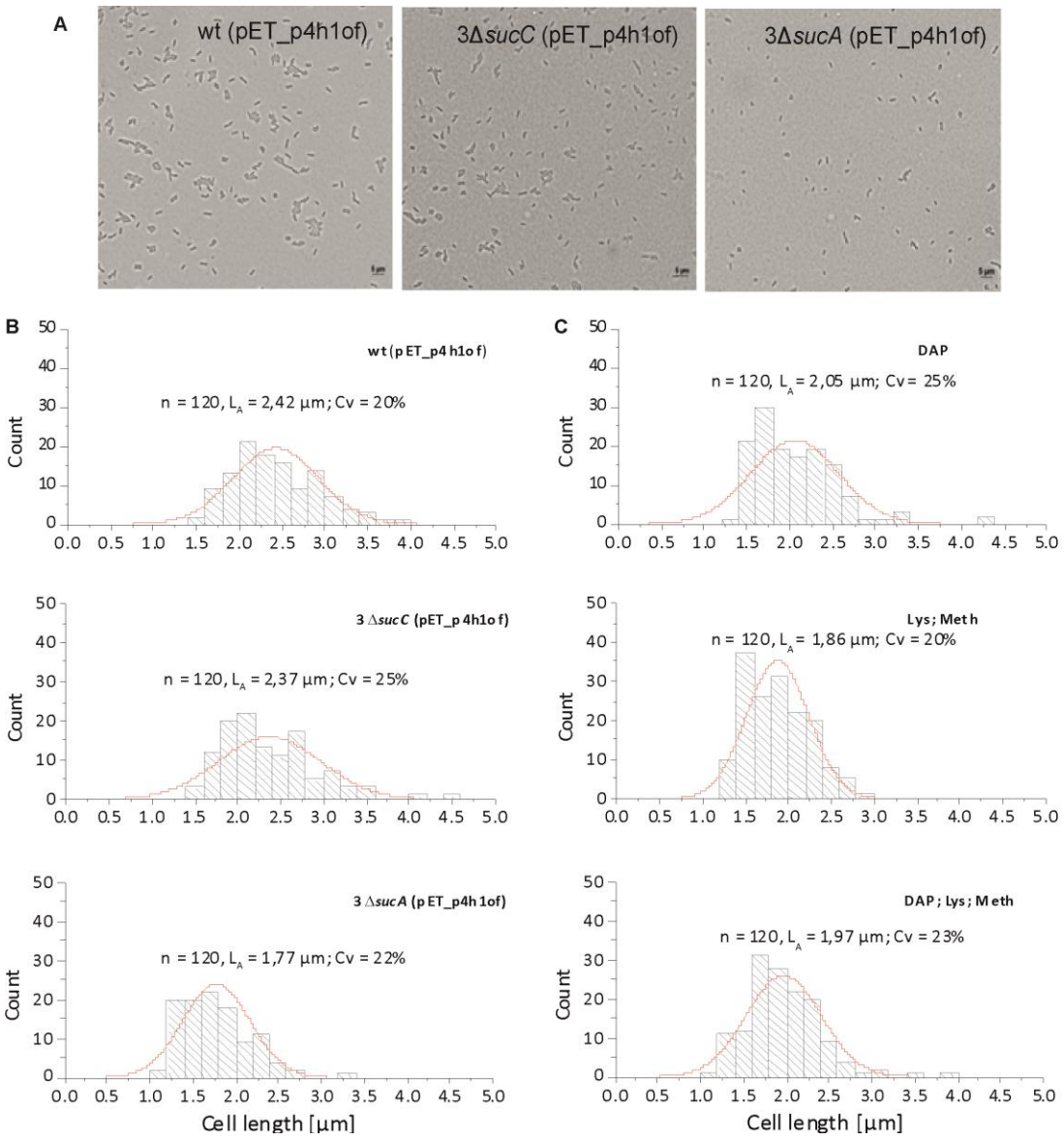

Figure 4